Supporting Information for "Sediments in sea ice drive the Canada Basin surface Mn maximum: insights from an Arctic Mn ocean model"

B. Rogalla[1], S. E. Allen[1], M. Colombo[1], P. G. Myers[2], K. J. Orians[1]

[1]Department of Earth, Ocean, and Atmospheric Sciences, University of British Columbia, Vancouver, British Columbia V6T1Z4,

Canada

[2]Department of Earth and Atmospheric Sciences, University of Alberta, 1-26 ESB, Edmonton, Alberta T6G2E3, Canada

Contents of this file

1. Text S1 to S2

2. Figures S1 to S12

3. Table S1 to S2

Corresponding author: B. Rogalla, Department of Earth, Ocean, and Atmospheric Sciences, University of British Columbia, Earth Sciences Building, Vancouver BC V6T1Z4, Canada. (brogalla@eoas.ubc.ca)

Text S1. Reversible Scavenging parameterization details. Dissolved Mn adsorbs to particle surfaces (pMn) and oxidises to oMn forming larger aggregates which sink. dMn is regenerated through the release of Mn from particles through desorption and by the reduction of oMn. These processes constitute the reversible scavenging of Mn and can be represented as follows (expanded from Van Hulten et al., 2017):

$$\frac{\partial [dMn]}{\partial t} = -k_{ox} \cdot [dMn] + k_{re} \cdot [oMn] - k_{ad} \cdot [dMn] + k_{de} \cdot [pMn] + physics + S \quad (1)$$

$$\frac{\partial [pMn]}{\partial t} = k_{ad} \cdot [dMn] - k_{de} \cdot [pMn] - s_p \frac{\partial [pMn]}{\partial z} + physics + S \quad (2)$$

$$\frac{\partial [oMn]}{\partial t} = k_{ox} \cdot [dMn] - k_{re} \cdot [oMn] - s_{ox} \frac{\partial [oMn]}{\partial z} + physics + S \quad (3)$$

where s_p and s_{ox} are the pMn and oMn sinking rates, respectively, and k_{ad}, k_{ox}, k_{de}, and k_{re} are the rate constants for adsorption, oxidation, desorption, and reduction. The physics term represents mixing and advection processes, and S represents the contribution from sources and sinks. Away from sources and sinks, assuming steady state, negligible impact of mixing and advection, and a weak vertical gradient in Mn concentrations, the equations are decoupled and we can estimate the scavenging rates from Eqn. 2 and 3:

$$[dMn] = \frac{k_{re}}{k_{ox}} \cdot [oMn] \quad (4)$$

$$[dMn] = \frac{k_{de}}{k_{ad}} \cdot [pMn] \quad (5)$$

Using Mn observations from the Canadian Arctic (Colombo et al., 2020; Li, 2017), we estimate the background scavenging rates for oxidation and adsorption, k_p, and for reduction and desorption, k_d, from the ratio of dissolved and particulate Mn concentrations. We consider only observations from regions far away from coastal processes and the ocean surface where the assumptions hold. This condition reduces the available observations to

those from stations in deeper areas of Baffin Bay and Canada Basin (Fig. S1) which have relatively small particle fluxes and are far away from sources. We match observations of dissolved and particulate Mn at equal depths and fit a linear regression through the origin (Fig. S2). Using this method, the ratio of scavenging rates, k_p/k_d, is estimated to be 1.48 ± 0.1 and with a k_d of $4.72 \cdot 10^{-7}$ s^{-1} (Bruland et al., 1994), k_p is estimated as $7.00 \cdot 10^{-7}$ s^{-1}.

Since we model dMn and oMn, while taking into account only the indirect effect of particle-bound Mn on dissolved Mn concentrations (included in the S source and sink term), the final reversible scavenging equations in our Mn model are:

$$\frac{\partial [dMn]}{\partial t} = -k_p \cdot [dMn] + k_d \cdot [oMn] + physics + S \tag{6}$$

$$\frac{\partial [oMn]}{\partial t} = k_p \cdot [dMn] - k_d \cdot [oMn] - s_{ox}\frac{\partial [oMn]}{\partial z} + physics + S \tag{7}$$

These equations do not incorporate a dependence on the dissolved oxygen concentration since Arctic waters are generally well oxygenated.

Text S2. Calculation of Net Mn transport through Parry Channel. In this study, we calculated net Mn transport from Canada Basin into Parry Channel and from Parry Channel into Baffin Bay via Lancaster Sound. The boundaries are defined along lines of constant i or j indices (Fig. S3). The Mn flux across each of the boundaries, ϕ_{bdy}, is the sum of the dissolved Mn concentration at the boundary grid points with indices i, j, k, multiplied by the volume flux:

$$\phi_{bdy}(t) = \sum_{i,j,k}[dMn]_{i,j,k}(t) \cdot u_{i,j,k}(t) \cdot A_{i,j,k} \tag{8}$$

where u is the velocity perpendicular to the boundary at time, t, and A is the grid cell area. These time series were calculated from 5-day modelled velocity and tracer fields, interpolated onto the U grid.

Mn transport into and out of Parry Channel fluctuates seasonally, with a peak in the late summer (Fig. S4). The flux of Mn in the "clean" sea ice experiment is consistently smaller than for the experiment with sediment in sea ice. The upper bound river experiment has the highest transports of all the experiments. To compare the experiments, we calculate the percent contribution of the sea ice and river components to the net transport as follows:

$$p = (1 - \frac{\phi_{off}}{\phi_{on}}) \cdot 100\% \tag{9}$$

where ϕ_{off} is the Mn transport from an experiment with the relevant component "off". So, to estimate the sea ice contribution, we use the "clean" sea ice experiment for ϕ_{off} and to estimate the river contribution, we use the reference experiment (with lower bound rivers). ϕ_{on} is the Mn transport from an experiment with the component on, i.e. the reference experiment with dirty sea ice, and the upper bound river experiment, respectively. Based

on these calculations, the sediment released by sea ice contributes about 45% to the Mn transported from Canada Basin into Parry Channel and about 18% for the Mn transported from Parry Channel into Baffin Bay (Fig. S5). The sea ice contribution to Mn flux does not vary significantly between 2002-2019. Rivers account for 5-8% of the Mn transported into Parry Channel and 3-5% of the Mn transported from Parry Channel into Baffin Bay.
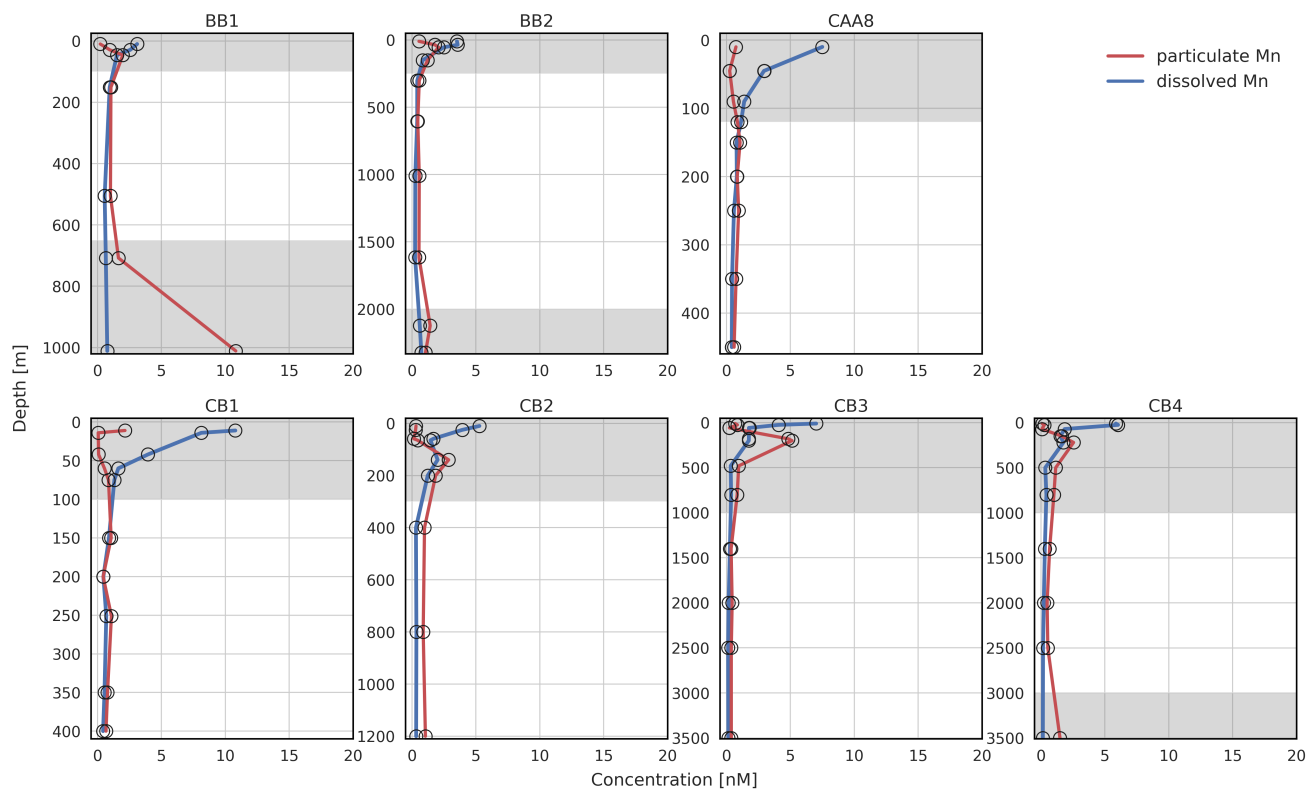
Figure S1. Profiles of dissolved Mn (blue) and particulate Mn (red), measured at stations in Baffin Bay, the Canadian Arctic Archipelago, and Canada Basin used for scavenging rate estimates. The depths at which sources affect the Mn concentrations are highlighted in gray and are excluded from the scavenging rate estimate. Note that the depth scale varies between plots.
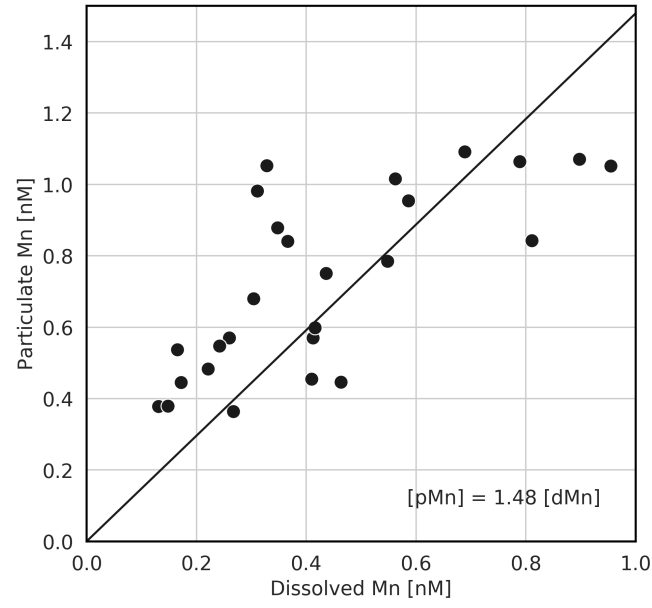
Figure S2.   Dissolved and particulate Mn observations measured at stations and depths away from Mn sources (profiles shown in Fig. S1). Measurements near the ocean surface and sea floor were removed. The data are linearly fit with a zero intercept (solid black line); the slope is 1.48 ± 0.10 [dMn] [pMn]$^{-1} = k_{de} \, (k_{ad})^{-1}$.
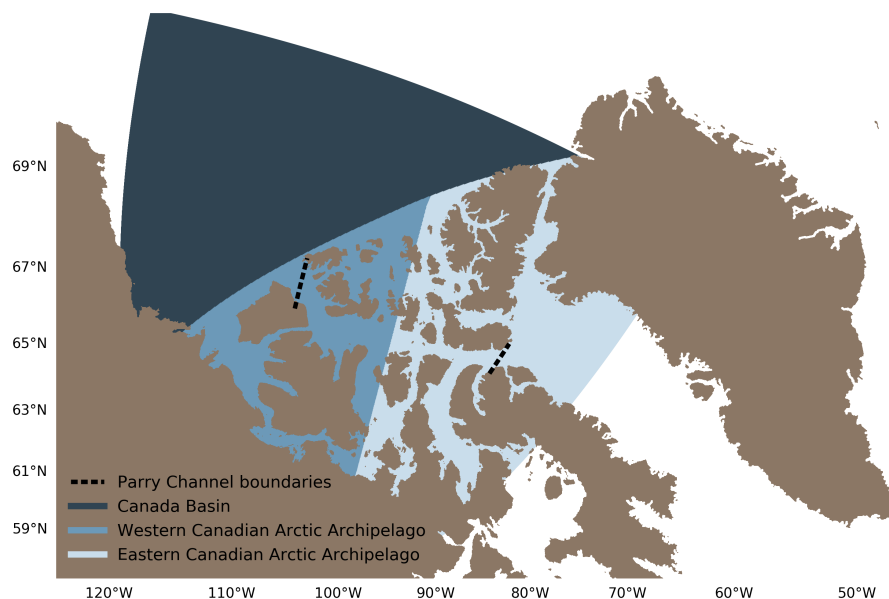
Figure S3.   Region definitions for the component contribution calculations in Table 2 and 3.
The boundaries indicated in black dashed lines were used for the calculations of net Mn transport
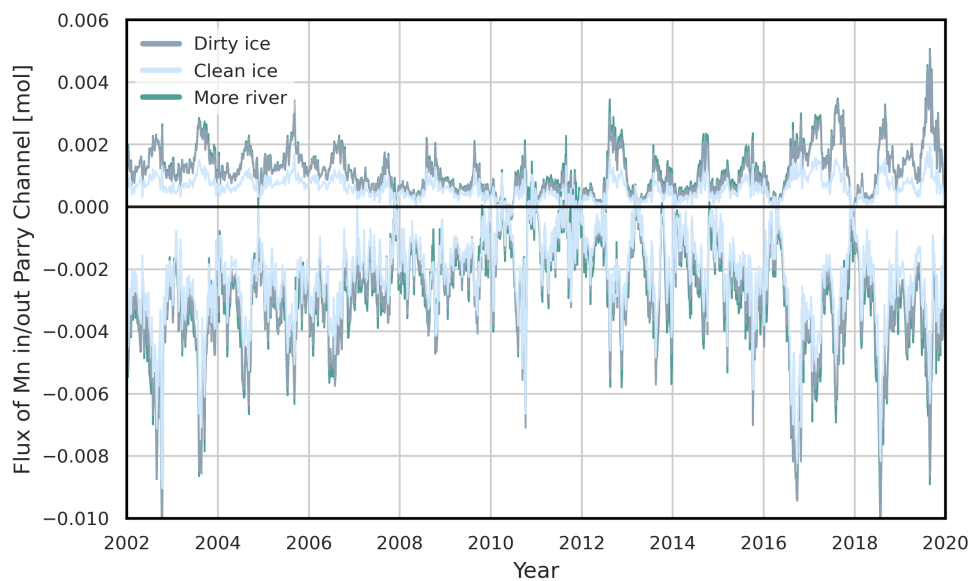into and of Parry Channel in Fig. S4 and S5.

Figure S4.   Net Mn flux into and out of Parry Channel along the boundaries defined in
Fig. S3. Positive flux represents transport into Parry Channel from Canada Basin. Negative
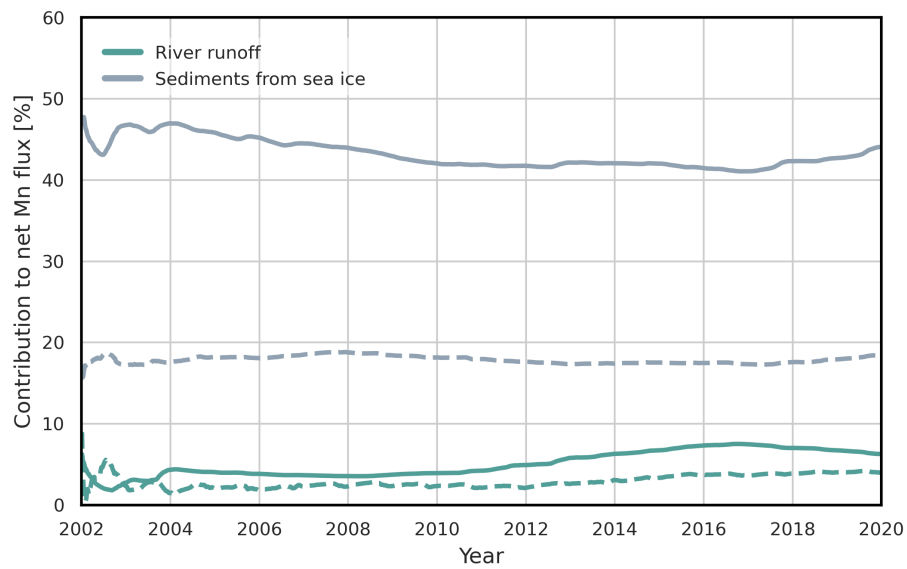flux is transport out of Parry Channel into Baffin Bay.

Figure S5. The percent contribution of sea ice melt and river runoff to net transport of Mn into and out of Parry Channel (boundaries shown in Fig. S3). Dashed lines correspond to the transport of Mn out of Parry Channel into Baffin Bay, while the solid lines are the transport of Mn from the Canada Basin into Parry Channel.
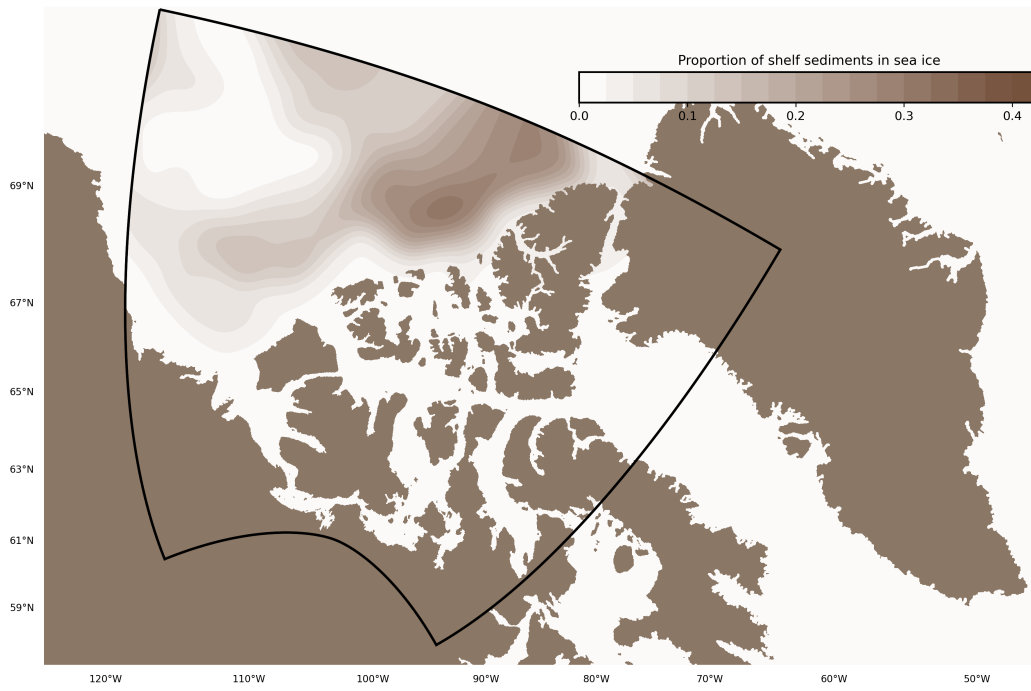
Figure S6.   The sediment content in sea ice in our model forcing is highest along the outer edges of Canada Basin, while the older sea ice at the core of the Beaufort Gyre is relatively "clean". The parameterization for sediment content in sea ice consists of a constant characteristic shelf sediment density, multiplied by the proportion of Siberian shelf-origin sediments found in sea ice in different regions (estimated from particle tracking).
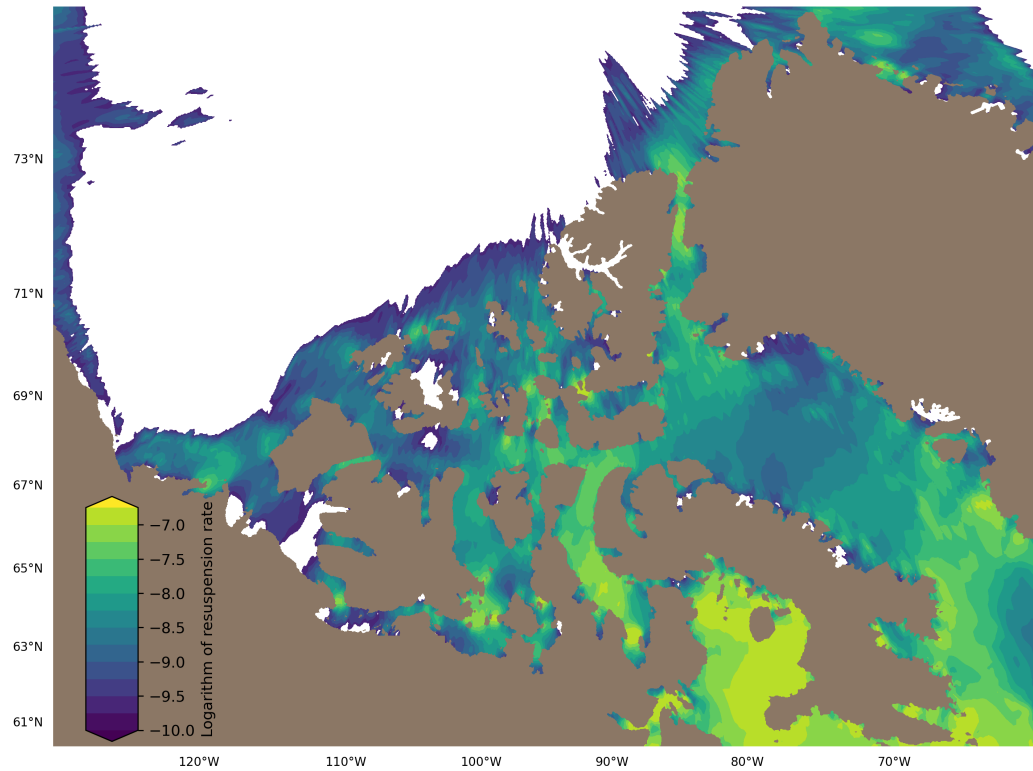
Figure S7. Erosion rate for Mn based on tidal speeds derived from the MOG2D-G model (Carrère and Lyard, 2003); the erosion rate is highest in the eastern Canadian Arctic Archipelago. Erosion rate is zero (white) in regions where tidal speeds are below 1 cm s^{-1}. Note that the colorbar scale is logarithmic.
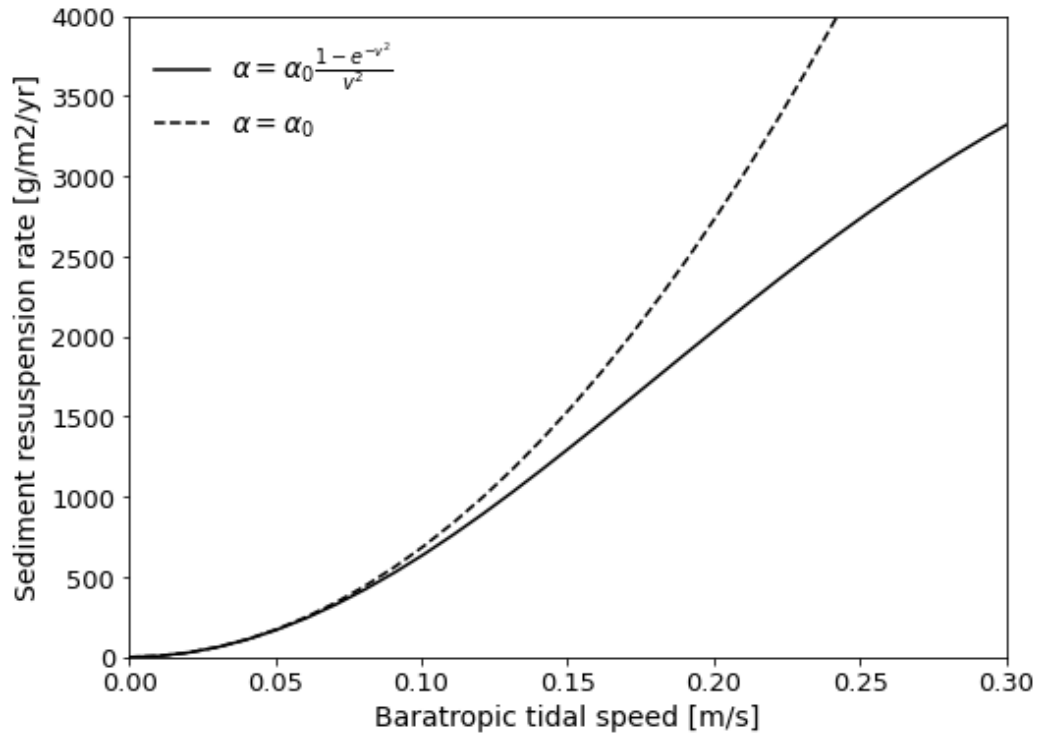
Figure S8. In our Mn model, the sediment resuspension rate is a function of the tidal speed, v, squared and is modulated by solubility, α, which is also a function of the tidal speed. In regions with strong tidal speeds, the readily available Mn has been dissolved from particles, and hence the solubility is reduced.
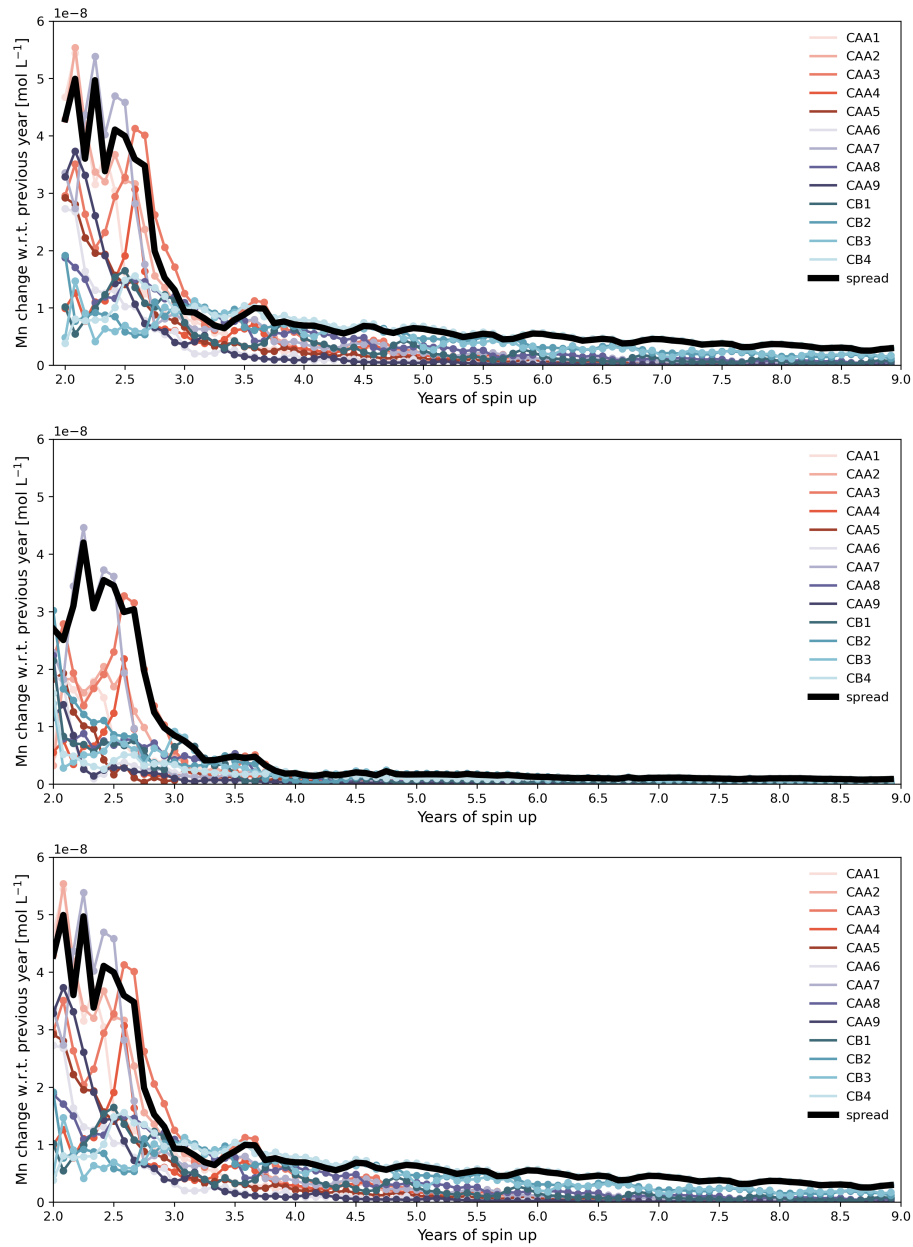
Figure S9.   For each simulation (top: reference, middle: "clean" sea ice, bottom: upper bound river), the Mn model is spun up by repeating the year 2002 until the year-to-year change in profile shape at evaluation stations is minimal. It takes about eight years to achieve spin-up, after which the full runs from 2002 to 2019 start. The "spread" is the difference between the maximum and minimum change at each month (solid black line). The legend includes the evaluation station names.
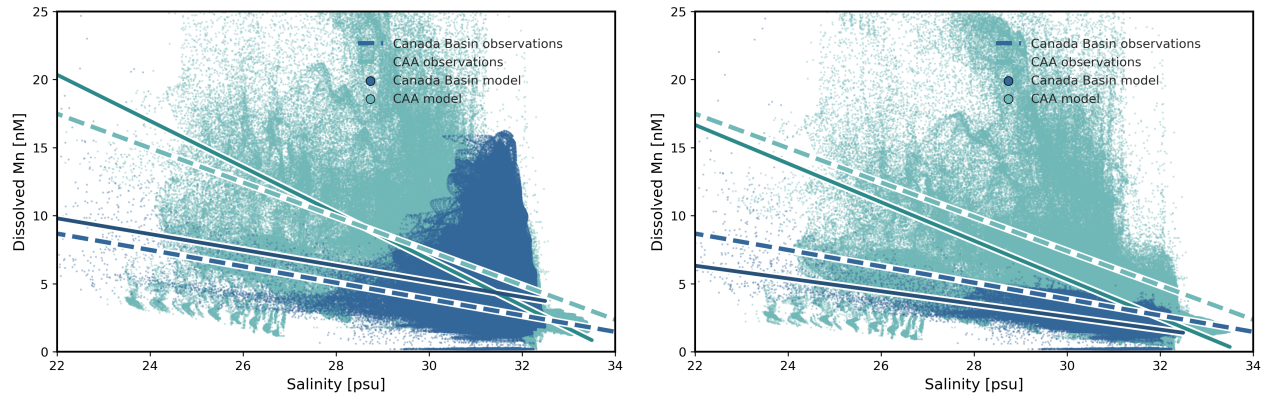
Figure S10. Monthly average model salinity and simulated dissolved Mn in September, 2015, in the Canada Basin and the Canadian Arctic Archipelago (CAA) for the two sea ice model experiments. We plot all modelled points for depths from 10-50 m from the reference run (left panel) and "clean" sea ice run (right panel) to compare the Mn-salinity relationship with observations (region separations defined in Fig. S3). The solid lines are linear regression fits for the model estimates in these regions from depths 10-50 m (depths coincide with observations). The dashed lines are fits from observations collected in the polar mixed layer in 2015 (Colombo et al., 2020). The overall representation of the low-salinity endmember is more accurate for the reference run than in the run without sediment in sea ice. The representation of regional differences is improved for both Canada Basin and the CAA in the reference run, although the CAA low-salinity endmember is slightly too high.
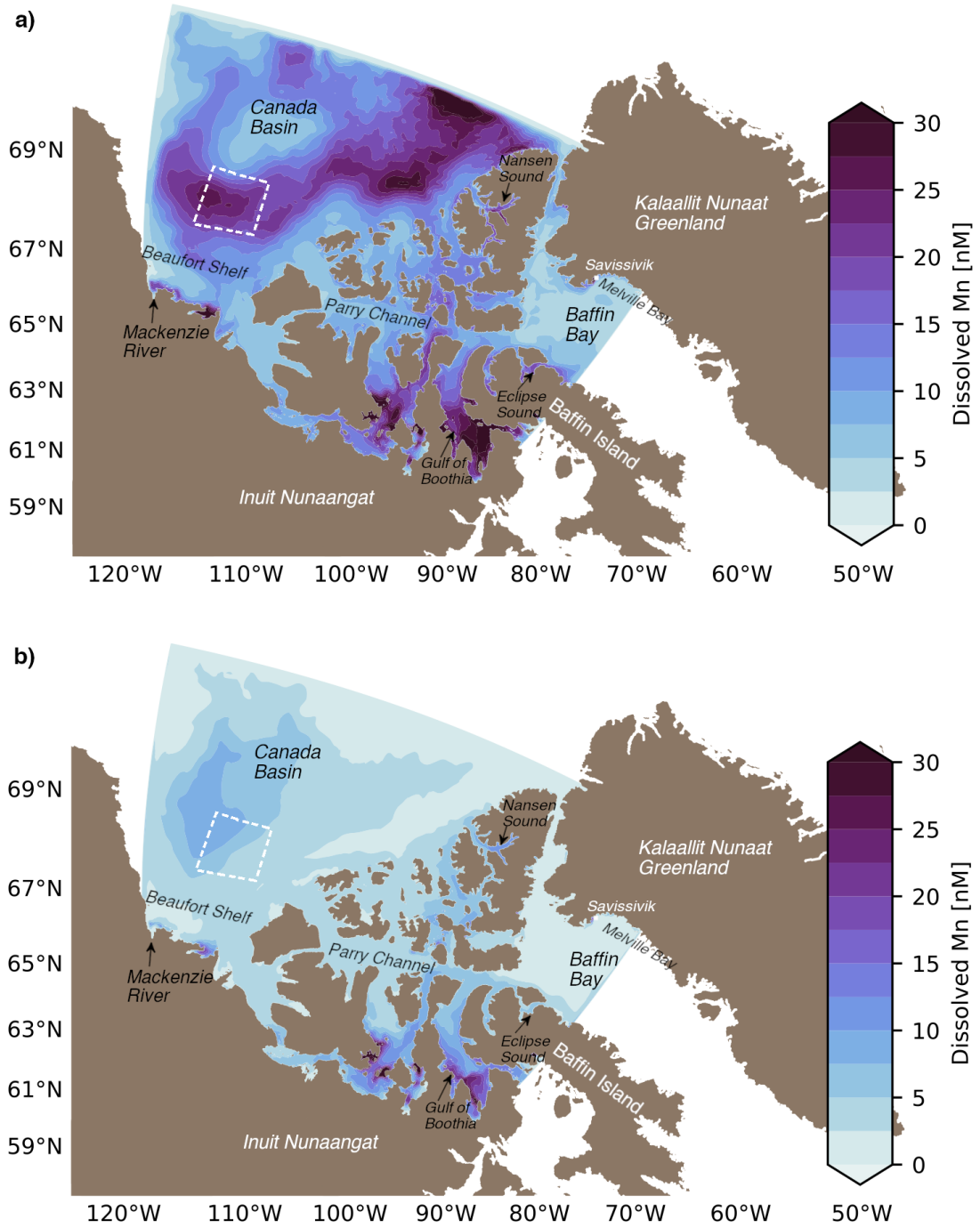
Figure S11. Simulated Mn concentrations in the upper 1 m in July, 2015 (a) and January, 2015 (b). The region outlined by a white dashed line is used to calculate a mean Mn profile with depth (Fig. S12). Note that the surface concentrations are much higher than for the polar mixed layer fields presented in Fig. 9.
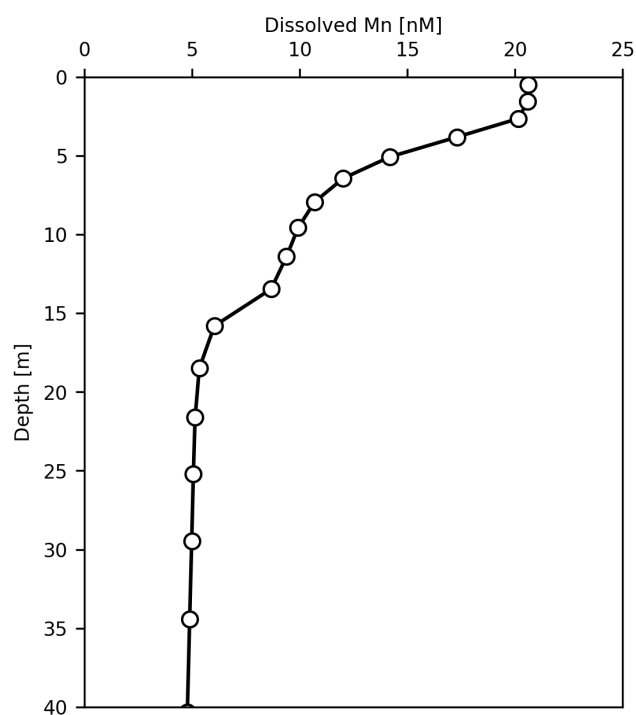
Figure S12.   Dissolved Mn concentrations are high at the surface and decrease strongly within the upper 5 m. This mean profile was calculated over a sub-region of the Canada Basin (dashed white line in Fig. S11). The markers indicate the model depth levels.

Table S1. A summary of average sediment loads and suspended particulate matter (SPM) concentrations measured in sea ice cores in the Arctic Ocean. The range of measured values are in brackets. Observed sediment content in sea ice is highly heterogeneous and can span multiple orders of magnitude. Where two estimates are given for the average content, the lower number is from "clean" ice cores and the higher number from turbid ice.

Sediment load (g m^{-2})	SPM (g m^{-3})	Location	Source
179 (0-972)	142 (24-192)	Laptev Sea	Eicken et al., 2000
-	149 (5-500+)	Lena delta	Hölemann et al., 1999
16 (9-46)	70 (8-600+)	Laptev sea	Eicken et al., 1997
-	45, 349 (0-964)	Laptev Sea	Nürnberg et al., 1994
(0-7000+)	-	NW of Alaska	Darby et al., 2011
128 (69-203)	342 (91-508)	Chukchi Sea	Eicken et al., 2005
232 (2-384)	564 (24-1474)	Alaska coast	Stierle et al., 2002
289	157 (31-593)	Beaufort Sea	Reimnitz et al., 1993
1400	-	Central Arctic	Darby et al., 2011
32 (8-84)	360 (7-2228)	Central Arctic	Tucker et al., 1999
-	68, 6800 (1-31013)	Central Arctic	Nürnberg et al., 1994
-	24 (0-725)	Fram Strait	Dethleff et al., 2010
-	11 (2-137)	Kara Sea	Dethleff et al., 2009

Table S2.   The spatial average annual dissolved Mn contributed by external model source components for the full water column (μmol m^{-2} yr^{-1}) in the reference experiment, averaged over the years 2002-2019, separated by region (Fig. S3). Sediment release by sea ice is the only component that varies significantly year-to-year. Estimates from the upper bound river contribution experiment are indicated in brackets.

Component contribution	Canada Basin		Canadian Arctic Archipelago	
	μmol m^{-2} yr^{-1}	%	μmol m^{-2} yr^{-1}	%
River discharge	5.2 (21)	2.7 (10)	15 (141)	1.1 (9.6)
Sediment resuspension	68	35 (33)	1284	96 (87)
Sediment from sea ice	120	62 (57)	44	3.3 (3.0)
Dust released by sea ice	0.2	0.1	0.3	0.0
Direct dust deposition	0.0	0.0	0.0	0.0
Total	193 (209)	100	1343 (1469)	100